

## Probing Intermolecular Interactions in Water/Ionic Liquid Mixtures by Far-infrared Spectroscopy

Ana Dominguez-Vidal,<sup>†</sup> Nina Kaun,<sup>†</sup> Maria Jose Ayora-Cañada,<sup>‡</sup> and Bernhard Lendl<sup>\*,†</sup>

*Institute of Chemical Technologies and Analytics, Vienna University of Technology, Getreidemarkt 9/164AC, A-1060 Wien, Austria, and Department of Physical and Analytical Chemistry, University of Jaén Campus "Las Lagunillas" S/N, E-23071 Jaén, Spain*

*Received: December 20, 2006; In Final Form: February 20, 2007*

Far-infrared spectra in the range from 600 to 20  $\text{cm}^{-1}$  of two hydrophilic (1-ethyl-3-methylimidazolium tetrafluoroborate and 1-butyl-3-methylimidazolium tetrafluoroborate) and one hydrophobic (1-butyl-3-methylimidazolium hexafluorophosphate) ionic liquids and their mixtures with water at different concentrations are reported. Shifts of the librational water bands depending on the nature of the anion are found to be related to the strength of the interaction between the water molecules and the anions. For both hydrophilic ionic liquids, the librational band is centered around 460  $\text{cm}^{-1}$ , whereas for the hydrophobic ionic liquid, it is shifted to 388  $\text{cm}^{-1}$ , indicating less hindered rotation of single water molecules. Multivariate curve resolution, paying special attention to the spectral range from 50 to 350  $\text{cm}^{-1}$ , was used to investigate the presence of different species with increasing water concentration. For both hydrophilic ionic liquids, a band located at 153  $\text{cm}^{-1}$  was resolved into two different contributions. A small contribution at 202  $\text{cm}^{-1}$  can be attributed to intermolecular interactions between water molecules forming dimers. The major contribution (centered at 148  $\text{cm}^{-1}$ ) corresponds to water molecules that do not bond to each other via H-bonding. It is therefore assigned to a hindered translation arising from the stretching of the hydrogen bond between  $\text{BF}_4^-$  anions and water molecules. Formation of water dimers in the hydrophobic ionic liquid does not occur. Furthermore, the spectral contribution of the stretching of H-bonds between water molecules and  $\text{PF}_6^-$  cannot be unambiguously detected, which indicates an extremely weak interaction between water molecules and this anion.

### 1. Introduction

Understanding the physical and chemical properties of water, and in particular the intermolecular hydrogen bonds, is considered a prerequisite for understanding biology and chemistry in aqueous solutions on a molecular level.<sup>1,2</sup> Investigation of the structural and binding properties of small water clusters and water complexes can provide a clue to the behavior of water and its role in such processes.

Vibrational spectroscopy is a powerful tool in studies of intermolecular interactions in condensed phases. The vibrational spectrum of liquid water<sup>3</sup> is traditionally divided into three different regions: (i) intramolecular vibrations above 1000  $\text{cm}^{-1}$ , (ii) the librational region from 300 to 1000  $\text{cm}^{-1}$ , and (iii) restricted translations from 0 to 300  $\text{cm}^{-1}$ . Especially in the latter region, the spectral information mainly derives from intermolecular water interactions, which have mostly been investigated so far by Raman spectroscopy.<sup>4,5</sup> Far-infrared (FIR) spectroscopy and terahertz (THz) spectroscopy are also valuable tools for gaining insight into processes in the liquid state on a molecular scale. These techniques are increasingly exploited to obtain information about interactions between water molecules themselves and with solutes when water is acting as a solvent. In this region, the water spectrum exhibits the following bands: The band around 180  $\text{cm}^{-1}$  can be considered as either stretching vibrations of an intermolecular  $\text{O}-\text{H}\cdots\text{O}$  bond or a translational motion.<sup>6,7</sup> The corresponding bending vibrations

of hydrogen bonds occur around 60  $\text{cm}^{-1}$  and are visible mainly by Raman spectroscopy and hardly by FIR spectroscopy.<sup>8,9</sup> The attribution of this band to  $\text{O}-\text{H}\cdots\text{O}$  hydrogen-bond stretching is supported by the fact that its absorbance increases upon cooling.<sup>10,11</sup> Furthermore, dielectric studies have shown an opposite effect, with the intensity of this band increasing upon heating. Thus, other contributions of relaxation processes (rotational or translational) of the water network have been considered.<sup>12,13</sup> In a complementary manner, the region of restricted translations is still influenced by the strong and broad libration band centered at 600  $\text{cm}^{-1}$ , which is assigned to hindered rotation of individual water molecules in a given water network. The whole water spectrum is strongly temperature-dependent,<sup>11</sup> and even small amounts of solutes can lead to noticeable changes.<sup>14</sup>

Recently, attention has been paid to the study of water dissolved in room-temperature ionic liquids (ILs), which are versatile solvents with a variety of research and industrial applications. Molecular dynamics simulations<sup>15,16</sup> and spectroscopic studies in the near-<sup>17</sup> and middle-<sup>18,19</sup> infrared regions have indicated that, in alkylimidazolium ionic liquids, water molecules tend to be isolated from each other. This is a consequence of the strong interactions between the water molecules and the anions of the ILs. Moreover, the association states of water in the three ionic liquids used in the present study were investigated by measuring in the OH stretching region at different water concentrations.<sup>20</sup> Self-association of water into dimers was found to occur in the studied hydrophilic ionic liquids but not in the hydrophobic IL.

\* Corresponding author. E-mail: blendl@mail.zserv.tuwien.ac.at.

<sup>†</sup> Vienna Institute of Technology.

<sup>‡</sup> University of Jaén.

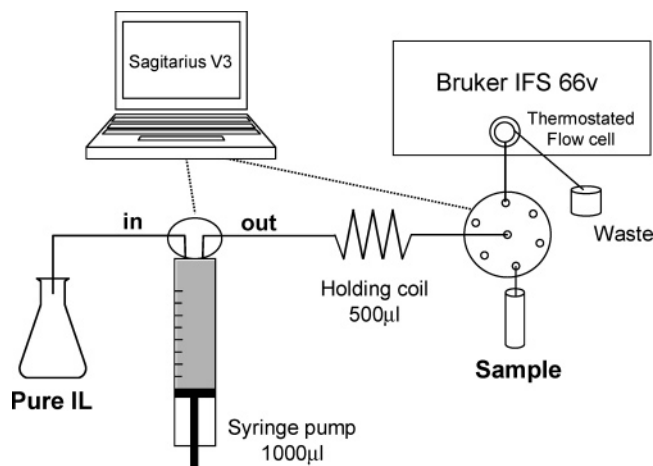


**Figure 1.** Sequential injection scheme employed for the on-line dilution of water/IL mixtures.

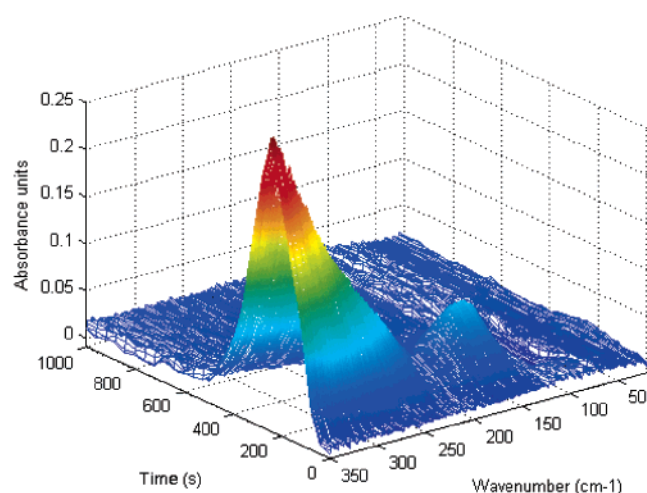


**Figure 2.** FIR spectra recorded by monitoring the on-line dilution of a water/bmimBF<sub>4</sub> mixture (5% w/w) using the described flow system.

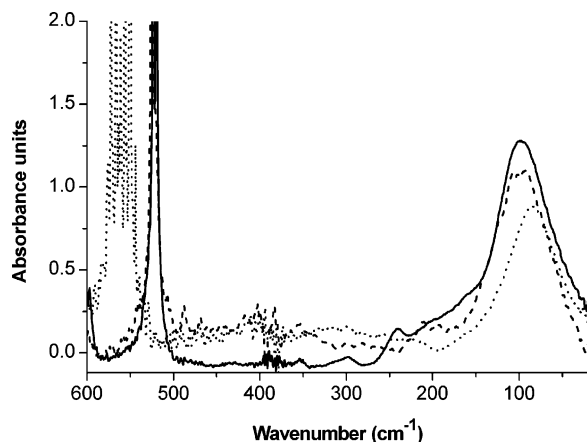


**Figure 3.** FIR spectra of emimBF<sub>4</sub> (solid line), bmimBF<sub>4</sub> (dash line), and bmimPF<sub>6</sub> (dotted line). All spectra have been corrected for beam intensity.

FIR spectra of isolated water molecules have been observed by measuring water diluted in a series of hydrophobic solvents.<sup>21</sup> That study revealed that the recorded spectral features of water essentially derived from the rotational motion of monomeric water in a solvent cage, with the rotation being more hindered in the less hydrophobic solvents.<sup>3,8,22</sup>

In this study, FIR spectra of water dissolved in three ILs at different concentrations have been recorded to gain more

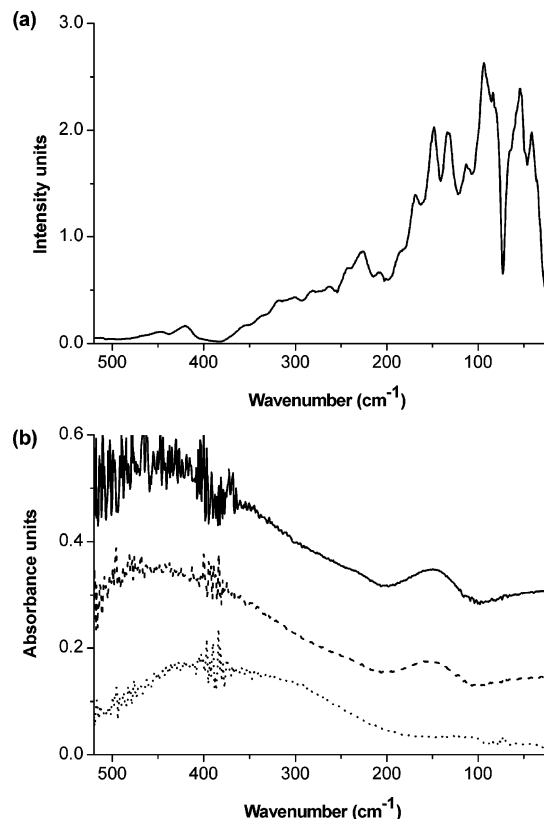


**Figure 4.** (a) Single-beam spectrum recorded with the empty PE cell. (b) Maximum FIR spectra obtained during on-line dilution with the flow system for 2% (w/w) water mixtures in emimBF<sub>4</sub> (solid line), bmimBF<sub>4</sub> (dashed line), and bmimPF<sub>6</sub> (dotted line). Spectra have been stacked for clarity.

information about the origin of the spectral features of water in the FIR spectral region. Two widely used hydrophilic ionic liquids (1-ethyl-3-methylimidazolium tetrafluoroborate and 1-butyl-3-methylimidazolium tetrafluoroborate) and a hydrophobic one (1-butyl-3-methylimidazolium hexafluorophosphate) were chosen. In addition, the FIR spectra of the pure ionic liquids are reported for the first time. Multivariate curve resolution analysis was employed to retrieve the pure spectra and concentration profiles of the different species.

## 2. Experimental Section

**Chemicals.** 1-Butyl-3-methylimidazolium hexafluorophosphate (bmimPF<sub>6</sub>), 1-butyl-3-methylimidazolium tetrafluoroborate (bmimBF<sub>4</sub>), and 1-ethyl-3-methylimidazolium tetrafluoroborate (emimBF<sub>4</sub>) were purchased from Fluka (Steinheim, Germany) and used without further purification. Standard water/ionic liquid mixtures of 2 and 5 wt % were prepared gravimetrically. HPLC-grade water from Fluka was used for preparing the mixtures.

**Apparatus.** The flow system (Figure 1) was set up to include a Cervo (Sunnyvale, CA) XP 3000 syringe pump with a syringe of 1000 µL, a holding coil of 500 µL, and a Valco (Houston, TX) six-port selection valve equipped with an electronic microactuator. Teflon tubings (0.50 mm i.d.) were used. All tubings and fittings were obtained from Global FIA (Gig Harbor, WA). The flow system was computer controlled by custom software (Sagittarius V3).

Experiments were carried out at the IR Beamline at BESSY (Berlin, Germany)<sup>23</sup> using a Bruker IFS 66v spectrometer that allows for evacuation of the sample compartment. The instrument was equipped with a 6-µm-thick Mylar beam splitter coated with a germanium layer. Measurements were obtained

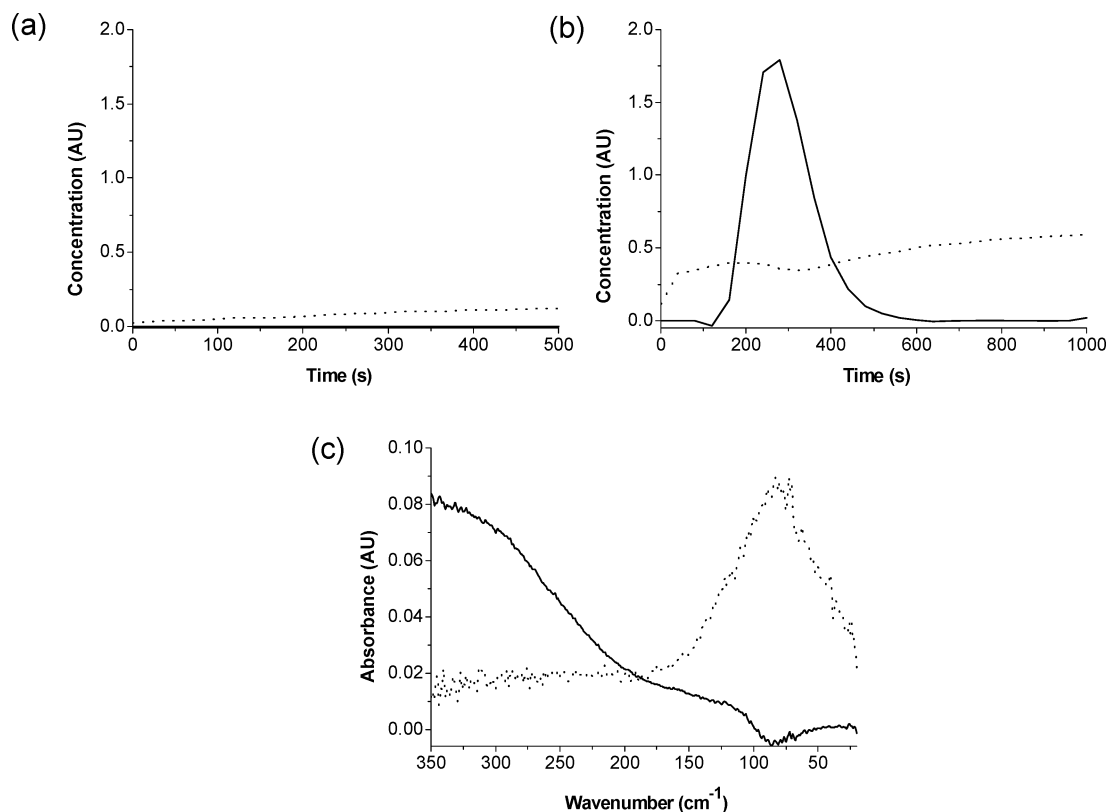


**Figure 5.** Results of MCR analysis of the augmented matrix for the experiments with bmimPF<sub>6</sub>. Recovered concentration profiles: (a) blank run and (b) on-line dilution of a 2% (w/w) water/bmimPF<sub>6</sub> mixture. (c) Pure spectra. Components: SIR decay contribution (dotted line) and water monomers interacting with IL anions (solid line).

in a water-thermostated flow-through cell (20 °C) equipped with 4-mm-thick polyethylene (PE) windows and a poly(tetrafluoroethylene) spacer providing an optical path length of 25  $\mu\text{m}$ . All spectra were recorded with a resolution of 1  $\text{cm}^{-1}$  as averages over 125 scans. Blackman-Harris three-term apodization and a scanner velocity of 60 kHz HeNe modulation frequency were used throughout. For detection, a He-cooled (4 K) bolometer was used. The experimental procedure did not allow for compensation of the intensity decay characteristic of synchrotron radiation sources. Compensation, however, was possible using multivariate curve resolution as explained in detail below.

**Experimental Procedures.** Standard mixtures containing 5% (w/w) water were prepared for emimBF<sub>4</sub> and bmimBF<sub>4</sub>. For bmimPF<sub>6</sub>, the maximum amount of water was 2% (w/w) because of the poor miscibility of the two liquids. Complete dissolution of water in each ionic liquid was assured.

Far-infrared spectra of the studied ILs containing different amounts of water were recorded using the above-described flow injection setup. This allowed for the measurement of different water concentrations in a simple and automated manner by means of reproducible on-line dilution of the standard mixtures.

For measurements, the flow system was flushed with dry ionic liquid, and a background spectrum was recorded. Then, a volume of 50  $\mu\text{L}$  of standard mixture was aspirated into the holding coil. Next, the flow was reversed to send the sample plug to the flow cell at a rate of 50  $\mu\text{L min}^{-1}$ . The dispersion produced during sample transport generated a concentration gradient of water.

Spectra were continuously recorded while the sample plugs passed the flow cell. Each spectrum acquisition took 37.5 s. In Figure 2, a three-dimensional plot of the spectra in the range of 350–20  $\text{cm}^{-1}$  is shown for one typical sample injection. It

should be noticed that, in this figure, the water concentration is a function of time as a consequence of the sample dispersion profile.

**Data Analysis.** Multivariate curve resolution—alternating least-squares is based on decomposition of the data obtained from the spectroscopic monitoring of a process into a concentration profile and a pure spectrum for each modeled component, following the model

$$\mathbf{D} = \mathbf{C}\mathbf{S}_T + \mathbf{E} \quad (1)$$

where  $\mathbf{D}$  is the matrix of spectral responses whose  $m$  rows are the number of spectra recorded during the process and whose  $n$  columns are the measured wavenumbers.  $\mathbf{C}$  represents the concentration profiles of the components during the experiment, and  $\mathbf{S}_T$  is the matrix of the pure spectra of these species.  $\mathbf{E}$  is the matrix of residuals not explained by the modeled components. The steps in MCR–ALS analysis of our data sets are summarized below.

(a) *Determination of the Number of Components.* Singular value decomposition (SVD)<sup>24</sup> was used for this purpose.

(b) *Initial Estimation of C Matrices.* Initial estimates of the  $\mathbf{C}$  matrices were obtained by evolving factor analysis (EFA).<sup>25</sup>

(c) *Optimization of the Initial Estimates.* The initial estimates of the  $\mathbf{C}$  matrices were optimized by an iterative alternating least-squares process. The addition of information in the optimization process helps to decrease the ambiguity in the results. This information is given by constraining the concentration profiles ( $\mathbf{C}$ ) and spectra ( $\mathbf{S}_T$ ) during the iterative optimization. A unimodality constraint was applied to the concentration profiles in this study.

The resolution process ends when the reproduced data matrix ( $\mathbf{D}^*$ ) obtained as the product of the resolved concentration

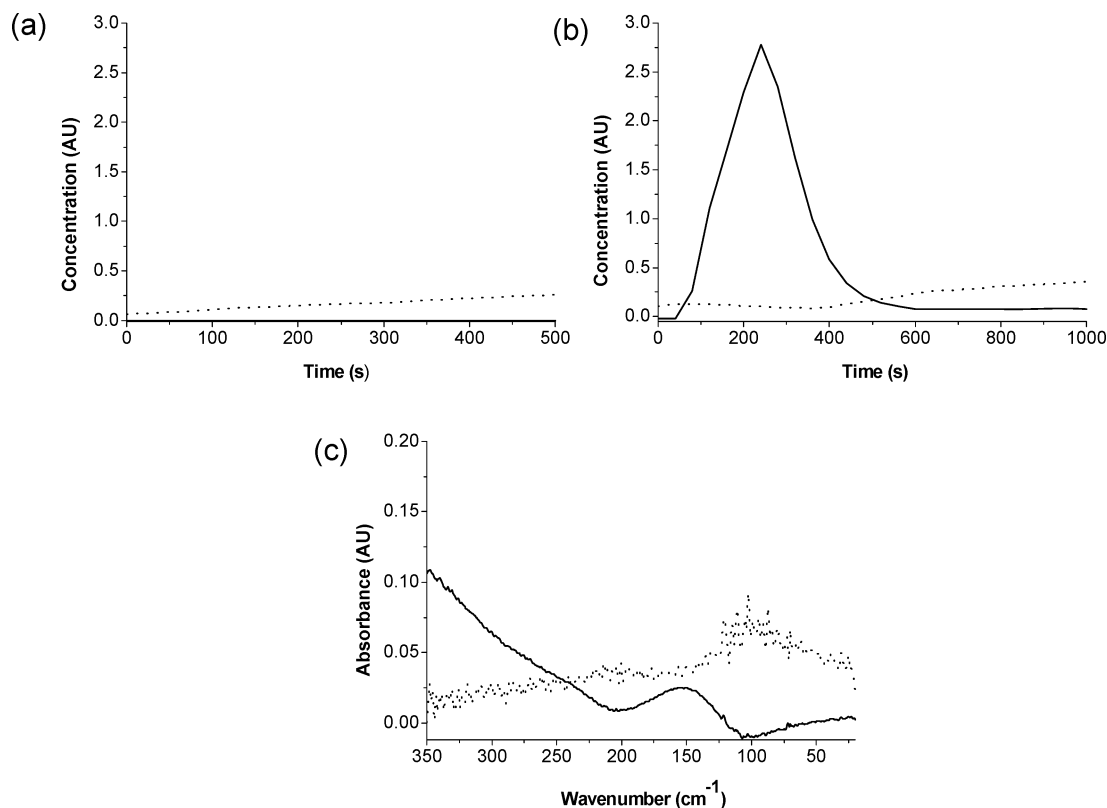


**Figure 6.** Results of MCR analysis of the augmented matrix for the experiments with bmimBF<sub>4</sub>. Concentration profiles: (a) blank run and (b) on-line dilution of a 5% (w/w) water/bmimBF<sub>4</sub> mixture. (c) Recovered pure spectra. Components: SIR decay contribution (dotted line) and water (solid line).

profiles (**C**) and spectra (**S<sub>T</sub>**) is sufficiently similar to the original matrix **D**. The optimal percent of lack of fit in relative standard deviation units is defined by eq 2 and compares the matrix obtained from the resolution results, **D**, with the experimental data

$$\% \text{ lack of fit} = 100 \times [(\sum r_{ij}^2)/(\sum d_{ij}^2)]^{1/2} \quad (2)$$

where  $d_{ij}$  designates an element of the data set **D** and  $r_{ij}$  is its related residual. Convergence is assumed to be fulfilled when the difference in fit between two consecutive iterations is less than 0.1%.

Sometimes, a single data matrix does not provide enough information to properly model the chemical system under study. In this situation, MCR-ALS can be applied to the simultaneous analysis of several matrices recorded under the same or different conditions. In this case, the individual matrices are arranged either in an augmented column-wise matrix (wavenumber-wise, keeping wavenumbers in common) or in an augmented row-wise matrix (time-wise, keeping time intervals in common). In our case, we used augmented column-wise matrices, consisting of two experiments: a blank experiment (blank run with only the corresponding pure ionic liquid) and a sample experiment (on-line dilution of a water/IL mixture). MCR-ALS analysis was performed in Matlab 7.0 (The Math Works Inc., Natick, MA, 1999) using the freely available program (Matlab code) by A. de Juan and R. Tauler.<sup>26</sup>

### 3. Results and Discussion

**Spectra of Water–Ionic Liquid Mixtures.** FIR spectra of pure emimBF<sub>4</sub>, bmimBF<sub>4</sub>, and bmimPF<sub>6</sub> in the range of 600–20 cm<sup>−1</sup> are presented in Figure 3. The spectra are mostly dependent on the anion, and two intense bands are clearly visible

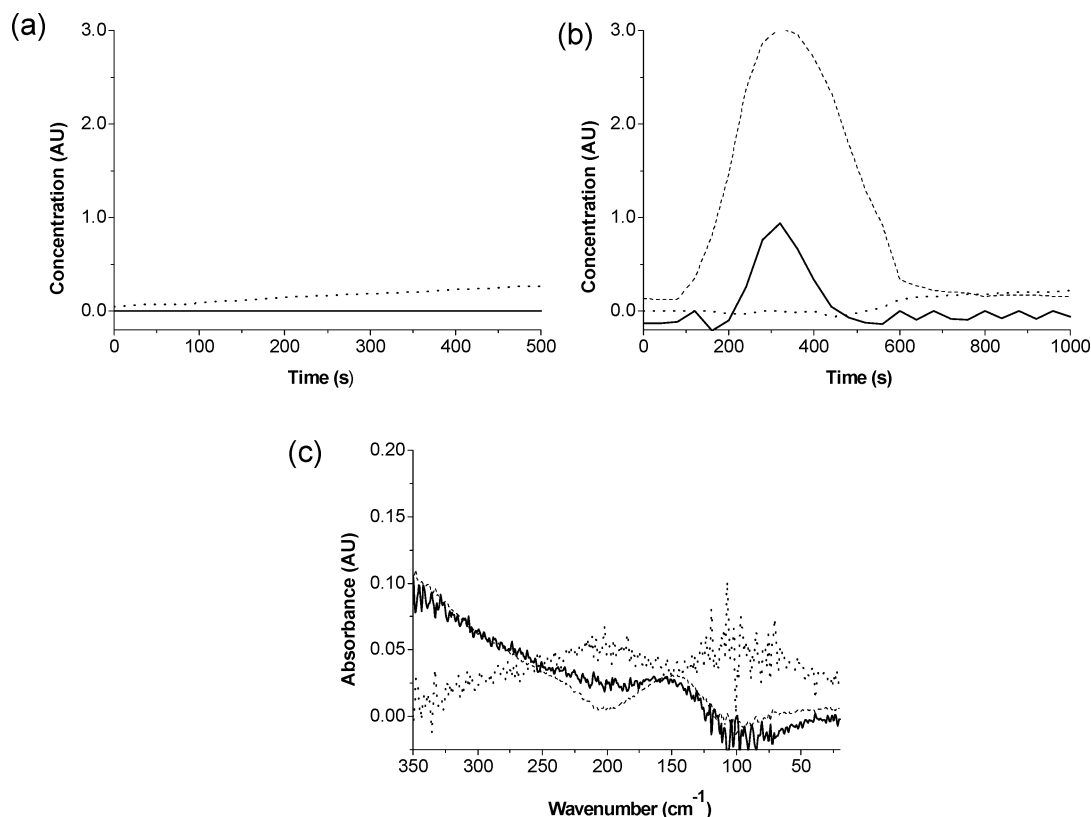
in all of them. The most intense band in emimBF<sub>4</sub> and bmimBF<sub>4</sub> (522 cm<sup>−1</sup>) can be assigned to tetrafluoroborate bending<sup>27</sup> ( $\delta$  BF<sub>4</sub><sup>−</sup>). The intense band at 562 cm<sup>−1</sup> in bmimPF<sub>6</sub> can be attributed to hexafluorophosphate bending<sup>28</sup> ( $\delta$  PF<sub>6</sub><sup>−</sup>). Bands at 98 and 83 cm<sup>−1</sup> can also be seen for the hydrophilic and hydrophobic ILs, respectively. Although no experimental infrared data of ILs below 200 cm<sup>−1</sup> are available yet in the literature, according to calculations, this region is dominated by cation–anion interactions (cation–anion bending).<sup>28</sup>

Figure 4a shows a single-beam spectrum recorded with the empty PE cell, and Figure 4b shows the typical spectra of water/IL mixtures with the dry IL recorded as background. Because of the low throughput at 380–400 cm<sup>−1</sup> as a result of the beam splitter employed, the recorded spectra showed an increased noise level in this spectral region. Furthermore, the range above 500 cm<sup>−1</sup> was not accessible with our setup because of the strong absorption of polyethylene and the ILs.

The spectra of water dissolved in the two BF<sub>4</sub><sup>−</sup>-based ionic liquids are very similar. The dominating feature is a wide band centered at around ~460 cm<sup>−1</sup> (here, only the low-frequency side of this band can be observed). A second band of lower intensity located at 149 cm<sup>−1</sup> for emimBF<sub>4</sub> and 151 cm<sup>−1</sup> for bmimBF<sub>4</sub> is also present. For bmimPF<sub>6</sub> the wide band appears at lower wavenumbers, centered at 388 cm<sup>−1</sup>.

Taking into account that the mid-infrared spectra of water dissolved in ionic liquids present features similar to those of water monomers in hydrophobic solvents,<sup>18</sup> far-infrared studies of monomeric water can be considered helpful in the interpretation of the FIR spectra reported here. Water dissolved in liquid cyclohexane<sup>21</sup> shows a broad asymmetric band (centered at 140 cm<sup>−1</sup>) that is attributed to the reorientational motion of the dipole of a freely rotating single water molecule in a solvent cage. Similar spectra have been obtained for other solvents. The





**Figure 7.** Results of MCR analysis of the augmented matrix for the experiments with emimBF<sub>4</sub>. Concentration profiles: (a) blank run and (b) on-line dilution of a 5% (w/w) water/emimBF<sub>4</sub> mixture. (c) Recovered pure spectra. Components: SIR decay contribution (dotted line), two water species (solid line and dashed line).

position of the band depends strongly on the nature of the solvent. In benzene, the least hydrophobic of the solvents studied, a broad band with a different shape and shifted to higher wavenumbers (230 cm<sup>-1</sup>) was observed. This experimental spectrum differed considerably from the calculated free rotation spectrum. The band of water in benzene was interpreted as a result of a more hindered rotational motion of the water molecule due to the collisions with the benzene rings. That study also refers to transient bands around 350–400 cm<sup>-1</sup> that were attributed to water clusters present in freshly prepared solutions that were not completely equilibrated. These bands disappeared when the solutions reached equilibrium. Thus, when the rotation of the water molecules becomes hindered, the band moves to higher wavenumbers; the more hindered, the higher the wavenumber until the known libration bands of liquid water.<sup>21</sup>

Considering these findings, hindered rotations (libration motions) of the water molecules interacting with the anions of the ionic liquid is the more plausible interpretation for the broad bands above 300 cm<sup>-1</sup> in the spectra presented here. This interaction has been found to occur with water acting as a double donor with the two H atoms forming two H-bonds.<sup>18</sup> Consequently, even though water is monomeric, the rotation is hindered, and the band is shifted to higher wavenumber with respect to that of the free rotating monomer. The higher position of this band in BF<sub>4</sub><sup>-</sup>-based ionic liquids (459 cm<sup>-1</sup>) compared to bmimPF<sub>6</sub> (388 cm<sup>-1</sup>) indicates that the rotation of the water molecules is more hindered in the former. This must be due to the fact that water molecules bind more strongly to BF<sub>4</sub><sup>-</sup> anions than to PF<sub>6</sub><sup>-</sup> anions. This finding agrees with the strengths of the H-bonds between water molecules and anions that were estimated from spectral shifts in the OH stretching region.<sup>18</sup>

Furthermore, rotation of the water monomers in the studied ionic liquids is less hindered than in the hydrogen-bonded network of liquid water (libration band centered at 670 cm<sup>-1</sup>).

Additionally, FIR spectra of water in BF<sub>4</sub><sup>-</sup>-based ILs present a band located at around 150 cm<sup>-1</sup>. In liquid water, the hydrogen-bond stretching mode is present in this spectral region, centered at about 200 cm<sup>-1</sup>.<sup>29</sup> In the mid-infrared study carried out by López et al. in our group,<sup>20</sup> formation of water dimers was found to occur in BF<sub>4</sub><sup>-</sup>-based ionic liquids but not in bmimPF<sub>6</sub>. Thus, water dimers could be responsible for this absorption, as this band is only present in tetrafluoroborate-based ionic liquids. The hypothesis of water dimers giving rise to the absorption at 148 cm<sup>-1</sup> in hydrophilic ionic liquids will be further investigated using chemometrics to study the evolution of the water spectra with increasing water concentration. By doing so, the presence of two different water species (monomers and dimers) could be detected and their pure FIR spectra recovered.

**Multivariate Curve Resolution-Alternating Least-Squares.** MCR–ALS was applied to extract pure concentration profiles and spectra of the different species present in the ILs. The spectral range from 350 to 20 cm<sup>-1</sup> was used to avoid the noise due to the beam splitter present above 350 cm<sup>-1</sup>. Considering that the experimental procedure did not compensate for the intensity decay characteristics of the synchrotron radiation sources, column matrix augmentation was always used to isolate this spectral contribution. For this purpose, an experiment involving pure IL without water addition was included in MCR analysis. The singular value decomposition of the column-wise combined matrices suggests the existence of two components contributing to the system in bmimPF<sub>6</sub> and bminBF<sub>4</sub>, whereas three components were found for emimBF<sub>4</sub>.

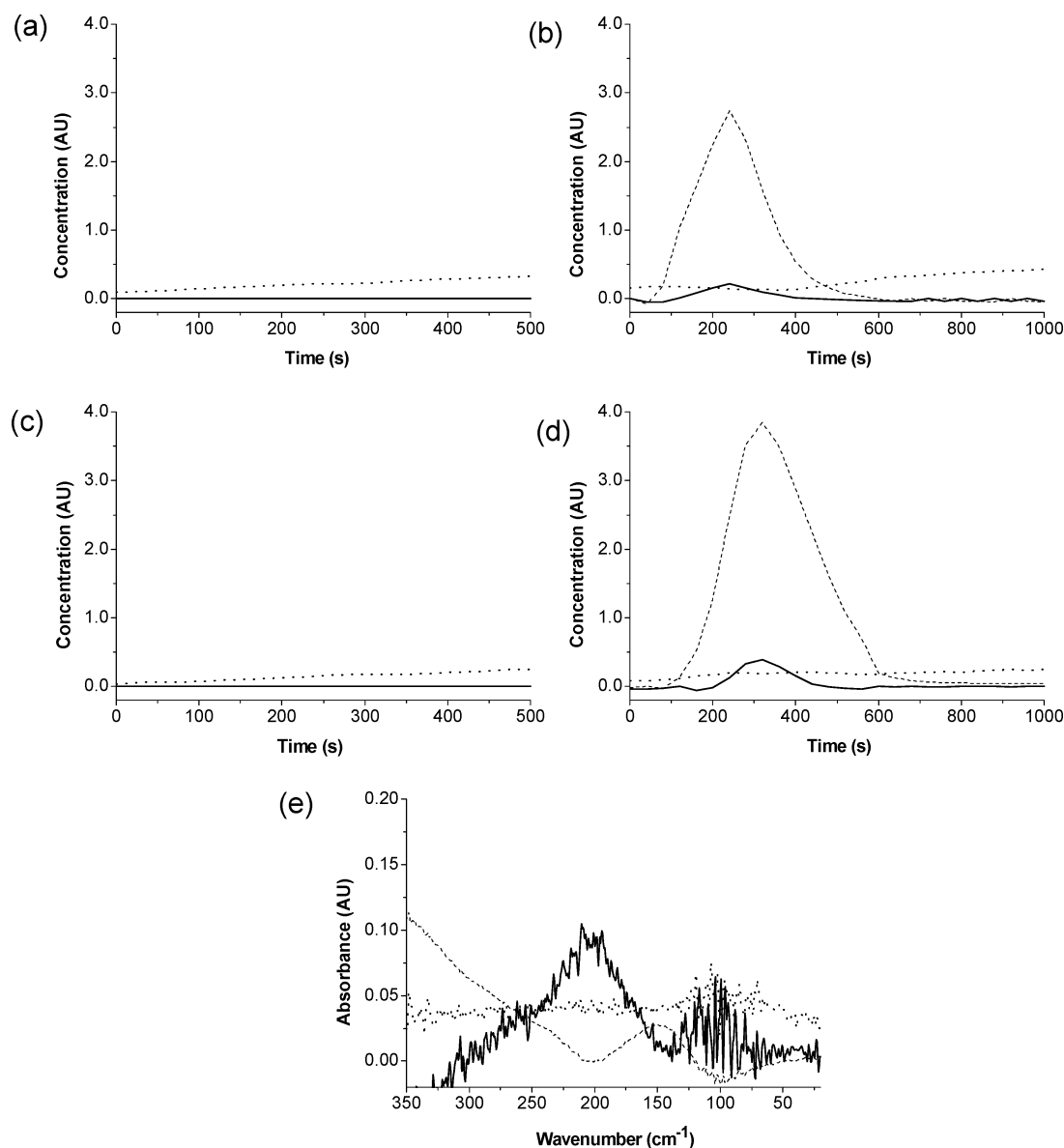


**Figure 8.** Results of MCR analysis of the augmented matrix for the experiments with both hydrophilic ionic liquids. Concentration profiles: (a) bmimBF<sub>4</sub> blank run, (b) on-line dilution of a 5% (w/w) water/bmimBF<sub>4</sub> mixture, (c) emimBF<sub>4</sub> blank run, (d) on-line dilution of a 5% (w/w) water/emimBF<sub>4</sub> mixture. (e) Recovered pure spectra. Components: SIR decay contribution (dotted line), two water species (solid line and dashed line).

Figures 5–7 show MCR results (concentration profiles and pure spectra of the detected components) for bmimPF<sub>6</sub>, bminBF<sub>4</sub>, and emimBF<sub>4</sub>, respectively. In all cases, one component can be attributed to the continuous absorbance increase due to synchrotron infrared radiation (SIR) decay, which is reflected in an increase of the baseline and the IL absorption. The spectra of this component present features in the region of ILs and noise. A second component presents the typical shape of a dispersion profile generated by the insertion of the water sample in the flow system. The recovered spectra correspond to those already described for water in the respective ILs.

For emimBF<sub>4</sub>, an additional component was found. Its spectrum (see Figure 7c) presents features similar to those of the second component described above. It seems to be a minor water species, because the spectrum is noisier and the concentration profile is less intense. This spectrum shows a higher intensity in the range of 200 cm<sup>-1</sup>, and the maximum of the shoulder is slightly shifted to higher wavenumbers (154 vs 147 cm<sup>-1</sup>).

The different behavior between bmimBF<sub>4</sub> and emimBF<sub>4</sub> does not agree with the similarities in the presented spectra (Figure

4) and the established knowledge about the water–IL interaction, which is said to be mostly dependent on the anion. Furthermore, in the reported mid-infrared study,<sup>20</sup> the second species of water was found in bmimBF<sub>4</sub> as well, although it formed at higher water/IL molar ratios than in emimBF<sub>4</sub>. This might be the reason why the second species is not well resolved in this ionic liquid. To improve the resolution, experiments from the two hydrophilic ILs were analyzed together by means of column-wise matrix augmentation. Three components were used to model the system. Figure 8 shows the results.

Two species of water were now detected in bmimBF<sub>4</sub> as well, and the resolution of their spectra was improved. The major component must be attributed to monomeric water interacting with the anions of the IL because it is present even at low water concentrations. This means that the band at 148 cm<sup>-1</sup> cannot be explained by H-bond interactions between water molecules. This band must come from a hindered translational motion (stretch) of the water monomers H-bonded to the anions of the IL.

The minor component appears only at higher water concentrations and presents a unique band located at ca. 202 cm<sup>-1</sup>.

This component shows a high level of noise because of its very low contribution. This species of water, which is observed only in hydrophilic ILs, must come from water dimers, and its recovered FIR spectrum essentially originates from the stretching mode of the O—H...O bond located around 200 cm<sup>-1</sup>. This assignment is in agreement with the study of Brubach et al., who found that only the middle region ( $150 \leq \omega \leq 300$  cm<sup>-1</sup>) of the so-called connectivity band in liquid water is related to changes in hydrogen bonding<sup>10</sup> and to the computed FIR spectrum of superheated steam,<sup>21,30</sup> which showed water dimer features around 200 cm<sup>-1</sup>. Furthermore, in the latter study, it was found that the high-frequency libration mode of the dimers was too weak to be visible.

Comparing the results obtained for the BF<sub>4</sub><sup>-</sup>-based ionic liquids to those obtained for bmimPF<sub>6</sub>, it is interesting to point out that the translational band attributed to the interaction between monomeric water and the anions is absent in bmimPF<sub>6</sub> spectra. This could be an indication that no H-bond is formed between water and PF<sub>6</sub><sup>-</sup> anions, which corroborates the results of a very recent theoretical study.<sup>31</sup> Wang et al. found that, in contrast to BF<sub>4</sub><sup>-</sup> anions, hydrophobic PF<sub>6</sub><sup>-</sup> anions could not form a stable complex with the water molecules at the density functional theory (DFT) level. Nevertheless, considering the recovered spectrum of bmimPF<sub>6</sub> (Figure 5c) in detail, despite the probable rotational ambiguity in MCR results and the overlapping with the IL band, a shoulder at around 115 cm<sup>-1</sup> might be seen. Its very weak intensity and the lower wavenumber position confirm a much weaker interaction between water and PF<sub>6</sub><sup>-</sup> anions compared to BF<sub>4</sub><sup>-</sup> anions.

## Conclusions

The librational band (above 300 cm<sup>-1</sup>) is the most intense spectral feature in the far-infrared spectra of water monomers in water/ionic liquid mixtures. The position of this band depends on the strength of the interaction between water and the ionic liquid. The stronger the interaction, the higher the position of the band, reflecting more hindered rotational motions. In BF<sub>4</sub><sup>-</sup>-based ionic liquids, the translational bands also found below 200 cm<sup>-1</sup> were attributed to the stretching of the H-bonds between water and the anions. On the other hand, these bands cannot be clearly discerned in bmimPF<sub>6</sub>, indicating that the water/PF<sub>6</sub><sup>-</sup> interaction is very weak.

Furthermore, with the help of multivariate curve resolution, water dimers were detected only in hydrophilic ionic liquids. The retrieved pure spectrum of dimeric water showed a unique characteristic feature at 202 cm<sup>-1</sup>. Multivariate curve resolution was also helpful in modeling the spectral contribution of synchrotron radiation decay.

**Acknowledgment.** The authors are grateful to Dr. Ulrich Schade and Dr. Michele Ortolani for fruitful discussions and their support at the IR Beamline BESSY. This work was supported further by the European Community-Research Infrastructure Action under the FP6 "Structuring the European

Research Area" Programme (through the Integrated Infrastructure Initiative "Integrating Activity on Synchrotron and Free Electron Laser Science", Contract R II 3-CT-2004-506008). A.D.V. is also grateful to the Spanish Ministry of Education and Science for a postdoctoral grant. N.K. was financially supported by the Austrian Science Fund within Project FWF 15531.

## References and Notes

- (1) Ronne, C.; Astrand, P.-O.; Keiding, S. R. *Phys. Rev. Lett.* **1999**, *82*, 2888.
- (2) Matei, A.; Dressel, M. J. *Biol. Phys.* **2003**, *29*, 101.
- (3) Nielsen, O. F. *Annu. Rep. Prog. Chem. C: Phys. Chem.* **1993**, *90*, 3.
- (4) Amo, Y.; Tominaga, Y. *Physica A: Stat. Mech. Appl.* **2000**, *276*, 401.
- (5) Walrafen, G. E.; Chu, Y. C.; Piermarini, G. J. *J. Phys. Chem.* **1996**, *100*, 10363.
- (6) Gaiduk, V. I.; Vij, J. K. *Phys. Chem. Chem. Phys.* **2001**, *3*, 5173.
- (7) Walrafen, G. E.; Chu, Y. C.; Piermarini, G. J. *J. Phys. Chem.* **1996**, *100*, 10363.
- (8) Hasted, J. B.; Husain, S. K.; Frescura, F. A. M.; Birch, J. R. *Chem. Phys. Lett.* **1985**, *118*, 622.
- (9) Nielsen, O. F. *Annu. Rep. Prog. Chem. C: Phys. Chem.* **1997**, *93*, 57.
- (10) Brubach, J. B.; Mermel, A.; Filabozzi, A.; Gerschel, A.; Roy, P. J. *Chem. Phys.* **2005**, *122*, 184509-1.
- (11) Zelsmann, H. R. *J. Mol. Struct.* **1995**, *350*, 95.
- (12) Ronne, C.; Keiding, S. R. *J. Mol. Liq.* **2002**, *101*, 199.
- (13) Vij, J. K.; Simpson, D. R. J.; Panarina, O. E. *J. Mol. Liq.* **2004**, *112*, 125.
- (14) Kaun, N.; Rodriguez Baena, J.; Newnham, D.; Lendl, B. *Appl. Spectrosc.* **2005**, *59*, 505.
- (15) Hanke, C. G.; Lynden-Bell, R. M. *J. Phys. Chem. B* **2003**, *107*, 10873.
- (16) Hanke, C. G.; Atamas, N. A.; Lynden-Bell, R. M. *Green Chem.* **2002**, *4*, 107.
- (17) Tran, C. D.; De Paoli Lacerda, S. H.; Oliveira, D. *Appl. Spectrosc.* **2003**, *57*, 152.
- (18) Cammarata, L.; Kazarian, S. G.; Salter, P. A.; Welton, T. *Phys. Chem. Chem. Phys.* **2001**, *3*, 5192.
- (19) Köddermann, T.; Wertz, C.; Heintz, A.; Ludwig, R. *Angew. Chem., Int. Ed.* **2006**, *45*, 3697.
- (20) López-Pastor, M.; Ayora-Cañada, M. J.; Valcárcel, M.; Lendl, B. *J. Phys. Chem. B* **2006**, *110*, 10896.
- (21) Tassaing, T.; Danten, Y.; Besnard, M. *Mol. Phys.* **1995**, *84*, 769.
- (22) Xu, J.; Plaxco, K. W.; Allen, S. J. *J. Chem. Phys.* **2006**, *124*, 036101.
- (23) Schade, U.; Roeseler, A.; Korte, E. H.; Bartl, F.; Hofmann, K. P.; Noll, T.; Peatman, W. B. *Rev. Sci. Instrum.* **2002**, *73*, 1568.
- (24) Golub, G. H.; Reinsch, C. *Numer. Math.* **1970**, *14*, 403.
- (25) Maeder, M.; Zuberbühler, A. D. *Anal. Chim. Acta* **1986**, *181*, 287.
- (26) Tauler, R.; de Juan, A. Multivariate Curve Resolution—Alternating Least Squares (MCR—ALS), MATLAB code; University of Barcelona: Barcelona, Spain, 1999.
- (27) Katsyuba, S. A.; Dyson, P. J.; Vandyukova, E. E.; Chernova, A. V.; Vidis, A. *Helv. Chim. Acta* **2004**, *87*, 2556.
- (28) Talaty, E. R.; Raja, S.; Storhaug, V. J.; Dölle, A.; Carper, W. R. *J. Phys. Chem. B* **2004**, *108*, 13177.
- (29) Guillot, B. *J. Chem. Phys.* **1991**, *95*, 1543.
- (30) Guillot B.; Guissani, Y. Simulation of the far infrared spectrum of liquid water and steam along the coexistence curve from the triple point to the critical point. In *NATO Series C: Mathematical and Physical Sciences. Collision and Interaction Induced Spectroscopy*; Tabisz, G. C., Neuman, M. N., Eds.; Kluwer Academic Publishers: Amsterdam, 1995; pp 129–142.
- (31) Wang, Y.; Li, H.; Han, S. *J. Phys. Chem. B* **2006**, *110*, 24646. s